

Splitting schemes for poroelasticity and thermoelasticity problems[☆]

Kolesov A.E.^a, Vabishchevich P.N.^{b,*}, Vasilyeva M.V.^a

^a*North-Eastern Federal University, Yakutsk, Russia*

^b*Nuclear Safety Institute, RAS, Moscow, Russia*

Abstract

In this work, we consider the coupled systems of linear unsteady partial differential equations, which arise in the modeling of poroelasticity processes. Stability estimates of weighted difference schemes for the coupled system of equations are presented. Approximation in space is based on the finite element method. We construct splitting schemes and give some numerical comparisons for typical poroelasticity problems. The results of numerical simulation of a 3D problem are presented. Special attention is given to using high performance computing systems.

Keywords: poroelasticity, thermoelasticity, splitting schemes, regularization, high performance computing

2000 MSC: 35Q74, 65M12, 65M60

1. Introduction

Poroelasticity [1, 2, 3, 4] and thermoelasticity problems [5, 6, 7, 8] are mathematically and physically analogous due to the fact that the pressure and temperature play a similar role in deformation of a body. For instance, a change in the temperature or a change in the pressure in a body results in equal normal strains in three orthogonal directions and no shear strains.

The basic mathematical models of such problems include the Lamé equation for the motion and the pressure/temperature equations. The fundamental point is that the system of equations is coupled: the equation for the motion includes the volume force, which is proportional to the temperature/pressure gradient, and the temperature/pressure equations include the term, which describes the compressibility of a medium.

To solve numerically the coupled quasi-stationary linear system of equations, we approximate our system using the finite element method [9, 10]. Variational formulations for poroelasticity and thermoelasticity problems and finite element approximations are considered in [11, 12, 13]. Due to the incompressibility constraint on the displacement field at

[☆]Supported by CJSC "OptoGaN" (contract N02.G25.31.0090); RFBR (project N13-01-00719A)

*Corresponding author

Email addresses: kolesov.svf@gmail.com (Kolesov A.E.), vabishchevich@gmail.com (Vabishchevich P.N.), vasilyevadotmdotv@gmail.com (Vasilyeva M.V.)

Preprint submitted to arXiv.org

November 20, 2021

the initial state (incompressible elasticity and Stokes type problem), the finite element interpolation with equal order spaces for both the displacement and pressure/temperature fields is not correct. It is well known that in classical mixed formulations, the finite element spaces must satisfy the LBB stability conditions [14, 15, 16]. These kind of discretizations for poroelasticity problems provides a lower order of convergence for the pressure in comparison with the displacements.

Quasi-stationary problem (steady for motion and unsteady for the temperature/pressure) is solved using the weighted scheme [17, 18]. The stability analysis is performed [19, 20] in the framework of the general theory of stability for operator-difference schemes [21, 22].

At present, different classes of additive operator-difference schemes for evolutionary equations are constructed via an additive representation of the main operator onto several terms. Additive schemes are constructed using splitting; they are associated with transition to a new time level on the basis of the solution of simpler problems for individual operators in the additive decomposition [23, 24]. We consider splitting (additive) schemes for poroelasticity/thermoelasticity problems with additive representation of the operator at the time derivative; we also consider modifications of splitting schemes. Similar schemes are examined in many studies [25, 26, 27, 28], but in our work, we show that these schemes are no more than regularization schemes [29, 24].

The work is organized as follows. Section 2 provides the mathematical model for the poroelasticity problem, which is the same as the thermoelasticity problem. In Section 3, we consider properties of the differential problem and give a priori estimates for the stability for the solutions with respect to initial the data and the right-hand side. In this section, we also formulate our problem as an initial value problem for a system of linear ordinary differential equations. Discretizations in space and in time are performed in Section 4. Here we conduct some analysis of the weighted differential schemes for coupled system. The central part of the work deals with the construction and numerical comparison of the stability of the splitting schemes. In Section 5, we consider the additive (splitting) schemes that are compared for typical poroelasticity problems in Section 7. Some modifications for additive (splitting) schemes associated with regularization are introduced in Section 6. The results of numerical simulation of a 3D problem on high performance computing systems are presented in Section 8.

2. Problem formulation

The linear poroelasticity equations can be expressed [1] as

$$\begin{aligned} \operatorname{div} \boldsymbol{\sigma}(\mathbf{u}) - \alpha \operatorname{grad}(p) &= 0, \\ \alpha \frac{\partial \operatorname{div} \mathbf{u}}{\partial t} + S \frac{\partial p}{\partial t} - \operatorname{div} \left(\frac{k}{\nu} \operatorname{grad} p \right) &= f(\mathbf{x}, t), \end{aligned} \quad (1)$$

with the boundary conditions

$$\begin{aligned} \boldsymbol{\sigma} \mathbf{n} &= 0, \quad \mathbf{x} \in \Gamma_N^u, \quad \mathbf{u} = 0, \quad \mathbf{x} \in \Gamma_D^u, \\ -\frac{k}{\nu} \frac{\partial p}{\partial n} &= 0, \quad \mathbf{x} \in \Gamma_N^p, \quad p = p_1, \quad \mathbf{x} \in \Gamma_D^p, \end{aligned} \quad (2)$$

and the initial conditions

$$p(\mathbf{x}, 0) = p_0, \quad \mathbf{x} \in \Omega. \quad (3)$$

Here the primary variables are the fluid pressure p and the displacement vector \mathbf{u} . Also, $\boldsymbol{\sigma}$ is the stress tensor, $S = 1/M$, M is the Biot modulus, k is the permeability, ν is the fluid viscosity, α is the Biot-Willis fluid/solid coupling coefficient and f is a source term representing injection or production processes. Body forces are neglected, \mathbf{n} is the unit normal to the boundary.

The stress tensor is given by

$$\boldsymbol{\sigma} = 2\mu\boldsymbol{\varepsilon}(\mathbf{u}) + \lambda \operatorname{div}(\mathbf{u}) \mathbf{I}, \quad (4)$$

where $\boldsymbol{\varepsilon}$ is the strain tensor:

$$\boldsymbol{\varepsilon}(\mathbf{u}) = \frac{1}{2} (\operatorname{grad} \mathbf{u} + \operatorname{grad} \mathbf{u}^T),$$

and μ, λ are Lamé coefficients, \mathbf{I} is the identity tensor.

In the case of thermoelasticity, the governing equations are the same as equations (1) [5, 6, 7, 8] with the temperature T instead of the pressure:

$$\begin{aligned} \operatorname{div} \boldsymbol{\sigma}(\mathbf{u}) - \beta \operatorname{grad}(T) &= 0, \\ \beta T_0 \frac{\partial \operatorname{div} \mathbf{u}}{\partial t} + c \frac{\partial T}{\partial t} - \operatorname{div}(\kappa \operatorname{grad} T) &= 0, \end{aligned} \quad (5)$$

where c is the heat capacity of the unit volume in the absence of deformation, κ is the thermal conductivity and β is the coupling coefficient playing the similar role as the Biot-Willis coefficient α . Here T_0 is the initial temperature of a medium.

3. Differential problem properties

We define the standard Hilbert space $H = L_2(\Omega)$ for the pressure with the following inner product and norm:

$$(u, v) = \int_{\Omega} u(\mathbf{x}) v(\mathbf{x}) dx, \quad \|u\| = (u, u)^{1/2}$$

and the Hilbert space $\mathbf{H} = (L_2(\Omega))^d$ for the displacement. Here $d = 2, 3$ is the number of spatial dimensions.

In H , we consider (see, e.g., \mathcal{A} [19, 20, 30]) the operator

$$\mathcal{A}v = -\mu \nabla^2 v - (\lambda + \mu) \operatorname{grad} \operatorname{div} v. \quad (6)$$

The operator \mathcal{A} is positive and self-adjoint in \mathbf{H} :

$$(\mathcal{A}v, v) \geq 0, \quad (\mathcal{A}v, u) = (v, \mathcal{A}u).$$

Similarly, in H , we define the operator \mathcal{B} as follows:

$$\mathcal{B}p = -\operatorname{div} \left(\frac{k}{\eta} \operatorname{grad} p \right). \quad (7)$$

The coupling terms in the poroelasticity problem are associated with the gradient and divergence operators denoted by \mathcal{G} and \mathcal{D} :

$$(\mathcal{G}p, \mathbf{u}) = -(\mathcal{D}\mathbf{u}, p). \quad (8)$$

Now equations (1) may be written in the operator-differential form as an abstract initial value problem:

$$\begin{aligned} \mathcal{A}\mathbf{u} + \alpha\mathcal{G}p &= 0, \\ \frac{d}{dt}(Sp + \alpha\mathcal{D}\mathbf{u}) + \mathcal{B}p &= f(t), \quad t > 0, \end{aligned} \quad (9)$$

with the initial condition for the pressure:

$$p(0) = p_0.$$

Let us define the inner products associated with \mathcal{A} and \mathcal{B} :

$$(u, v)_{\mathcal{A}} = (\mathcal{A}u, v), \quad (u, v)_{\mathcal{B}} = (\mathcal{B}u, v)$$

and the norms:

$$\|u\|_{\mathcal{A}} = (\mathcal{A}u, u)^{1/2}, \quad \|u\|_{\mathcal{B}} = (\mathcal{B}u, u)^{1/2}.$$

Theorem 1. *The solution of problem (9) satisfies the a priori estimate*

$$\|\mathbf{u}(t)\|_{\mathcal{A}}^2 + S\|p(t)\|^2 \leq \|\mathbf{u}(0)\|_{\mathcal{A}}^2 + S\|p(0)\|^2 + \frac{1}{2} \int_0^t \|f(s)\|_{\mathcal{B}^{-1}}^2 ds. \quad (10)$$

Proof. Multiplying the first and the second equations of (9) by $d\mathbf{u}/dt$ and p , respectively, we get

$$\begin{aligned} \left(\mathcal{A}\mathbf{u}, \frac{d\mathbf{u}}{dt} \right) + \alpha \left(\mathcal{G}p, \frac{d\mathbf{u}}{dt} \right) &= 0, \\ \frac{d}{dt}(S(p, p) + \alpha(\mathcal{D}\mathbf{u}, p)) + (\mathcal{B}p, p) &= (f, p). \end{aligned}$$

Adding this equations and using the relation (8), we obtain

$$\left(\mathcal{A}\mathbf{u}, \frac{d\mathbf{u}}{dt} \right) + S \left(p, \frac{dp}{dt} \right) + (\mathcal{B}p, p) = (f, p).$$

Using the Cauchy-Schwarz inequality for the right-hand side:

$$(f, p) \leq \|p\|_{\mathcal{B}}^2 + \frac{1}{4}\|f\|_{\mathcal{B}^{-1}}^2,$$

the following inequality is obtained:

$$\left(\mathcal{A}\mathbf{u}, \frac{d\mathbf{u}}{dt} \right) + S \left(p, \frac{dp}{dt} \right) \leq \frac{1}{4}\|f\|_{\mathcal{B}^{-1}}^2.$$

In view of

$$\left(\frac{d\mathbf{u}}{dt}, \mathbf{u} \right) = \frac{1}{2} \frac{d}{dt}(\mathbf{u}, \mathbf{u}),$$

we have

$$\frac{d}{dt} ((\mathcal{A}\mathbf{u}, \mathbf{u}) + S(p, p)) \leq \frac{1}{2} \|f\|_{\mathcal{B}^{-1}}^2.$$

Time integration gives the a priori estimate (10) providing stability with respect to the initial data and the right-hand side. \square

After differentiation with respect to time of the displacement equation, the operator-differential form of poroelasticity problem (9) may be written in a more convenient form:

$$\begin{aligned} \mathcal{A} \frac{d\mathbf{u}}{dt} + \alpha \mathcal{G} \frac{dp}{dt} &= 0, \\ \frac{d}{dt} (S p + \alpha \mathcal{D} \mathbf{u}) + \mathcal{B} p &= f(t), \quad t > 0, \end{aligned} \tag{11}$$

which is an initial value problem for a system of linear ordinary differential equations.

Let $\mathbf{U} = \{\mathbf{u}, p\}$ be the vector of unknowns, $\mathbf{F} = \{\mathbf{0}, f\}$ be the given vector of the right-hand sides and

$$\mathbb{B} \frac{d\mathbf{U}}{dt} + \mathbb{A} \mathbf{U} = \mathbf{F}, \quad t > 0, \tag{12}$$

with the initial conditions

$$\mathbf{U} = \mathbf{U}_0.$$

Here

$$\mathbb{B} = \begin{pmatrix} \mathcal{A} & \alpha \mathcal{G} \\ \alpha \mathcal{D} & S \mathcal{I} \end{pmatrix}, \quad \mathbb{A} = \begin{pmatrix} 0 & 0 \\ 0 & \mathcal{B} \end{pmatrix}. \tag{13}$$

Multiplying equation (12) by \mathbf{U} , we obtain

$$\frac{1}{2} \frac{d}{dt} (\mathbb{B} \mathbf{U}, \mathbf{U}) + (\mathbb{A} \mathbf{U}, \mathbf{U}) = (\mathbf{F}, \mathbf{U}).$$

For the right-hand side, we use the estimate

$$(\mathbf{F}, \mathbf{U}) \leq (\mathbb{A} \mathbf{U}, \mathbf{U}) + \frac{1}{4} (\mathbb{A}^{-1} \mathbf{F}, \mathbf{F}).$$

This provides the a priori estimate for the solution:

$$\|\mathbf{U}(t)\|_{\mathbb{B}}^2 \leq \|\mathbf{U}_0\|_{\mathbb{B}}^2 + \frac{1}{2} \int_0^t \|\mathbf{F}(s)\|_{\mathbb{A}^{-1}}^2 ds. \tag{14}$$

Note that this estimate is similar to the a priori estimate (10), but it is obtained in a more simple way.

4. Discretization in space and in time

For the numerical solution of the problem, first, we come to a variational problem by multiplying the first and the second equations of (1) by test functions \mathbf{v} and q ,

respectively, and integrating by parts to eliminate the second order derivatives. Find $\mathbf{u} \in \mathbf{V}$, $p \in Q$ such that

$$\begin{aligned} \int_{\Omega} \boldsymbol{\sigma}(\mathbf{u}) \boldsymbol{\varepsilon}(\mathbf{v}) dx + \int_{\Omega} \alpha(\operatorname{grad} p, \mathbf{v}) dx &= 0, \quad \forall \mathbf{v} \in \hat{\mathbf{V}}, \\ \int_{\Omega} \alpha \frac{d \operatorname{div} \mathbf{u}}{dt} q dx + \int_{\Omega} S \frac{dp}{dt} q dx + \int_{\Omega} \left(\frac{k}{\nu} \operatorname{grad} p, \operatorname{grad} q \right) dx \\ &= \int_{\Omega} f q dx, \quad \forall q \in \hat{Q}. \end{aligned} \quad (15)$$

Here the spaces of trial and test functions are defined as

$$\begin{aligned} \mathbf{V} &= \{ \mathbf{v} \in [H^1(\Omega)]^d : \mathbf{v}(\mathbf{x}) = 0, \mathbf{x} \in \Gamma_D^u \}, \\ \hat{\mathbf{V}} &= \{ \mathbf{v} \in [H^1(\Omega)]^d : \mathbf{v}(\mathbf{x}) = 0, \mathbf{x} \in \partial\Omega \}, \\ Q &= \{ q \in H^1(\Omega) : q(\mathbf{x}) = p_1, \mathbf{x} \in \Gamma_D^p \}, \\ \hat{Q} &= \{ q \in H^1(\Omega) : q(\mathbf{x}) = 0, \mathbf{x} \in \partial\Omega \}, \end{aligned}$$

where H^1 is a Sobolev space.

A discrete problem is obtained by restricting the variational problem (15) to pairs of discrete spaces of trial and test functions [11, 31]: find $\mathbf{u}_h \in \mathbf{V}_h \subset \mathbf{V}$, $p_h \in Q_h \subset Q$ such that

$$\begin{aligned} \int_{\Omega} \boldsymbol{\sigma}(\mathbf{u}_h) \boldsymbol{\varepsilon}(\mathbf{v}_h) dx + \int_{\Omega} \alpha(\operatorname{grad} p_h, \mathbf{v}_h) dx &= 0, \quad \forall \mathbf{v}_h \in \hat{\mathbf{V}}_h \subset \hat{\mathbf{V}}, \\ \int_{\Omega} \alpha \frac{d \operatorname{div} \mathbf{u}_h}{dt} q_h dx + \int_{\Omega} S \frac{dp_h}{dt} q_h dx + \int_{\Omega} \left(\frac{k}{\nu} \operatorname{grad} p_h, \operatorname{grad} q_h \right) dx \\ &= \int_{\Omega} f q_h dx, \quad \forall q_h \in \hat{Q}_h \subset \hat{Q}. \end{aligned} \quad (16)$$

For discretization in time, we employ the weighted difference scheme for time-stepping. We define the following bilinear and linear forms over the domain Ω :

$$\begin{aligned} a(\mathbf{u}, \mathbf{v}) &= \int_{\Omega} \boldsymbol{\sigma}(\mathbf{u}) \boldsymbol{\varepsilon}(\mathbf{v}) dx, \\ g(p, \mathbf{v}) &= \int_{\Omega} \alpha(\operatorname{grad} p, \mathbf{v}) dx, \\ c(p, q) &= \int_{\Omega} S p q dx, \\ d(\mathbf{u}, q) &= \int_{\Omega} \alpha \operatorname{div} \mathbf{u} q dx, \\ b(p, q) &= \int_{\Omega} \left(\frac{k}{\nu} \operatorname{grad} p, \operatorname{grad} q \right) dx, \\ l(f, q) &= \int_{\Omega} f q dx, \end{aligned}$$

Note that for all u and v , we have

$$d(u, v) = -g(v, u)$$

Let $\mathbf{u}^n = \mathbf{u}(\mathbf{x}, t_n)$, $p^n = p(\mathbf{x}, t_n)$, where $t_n = n\tau$, $n = 0, 1, \dots$, and $\tau > 0$. Then the problem is reformulated as follows: we search $p \in Q$ and $\mathbf{u} \in \mathbf{V}$ that satisfy the following relations:

for the displacement

$$a(\mathbf{u}^{n+1}, \mathbf{v}) + g(p^{n+1}, \mathbf{v}) = 0, \quad \forall \mathbf{v} \in \hat{\mathbf{V}}, \quad (17)$$

for the pressure

$$\begin{aligned} d\left(\frac{\mathbf{u}^{n+1} - \mathbf{u}^n}{\tau}, q\right) + c\left(\frac{p^{n+1} - p^n}{\tau}, q\right) \\ + b(p_\theta^{n+1}, q) = l(f_\theta^{n+1}, q), \quad \forall q \in \hat{Q}, \end{aligned} \quad (18)$$

with

$$\begin{aligned} p_\theta^{n+1} &= \theta p^{n+1} + (1 - \theta)p^n, \\ f_\theta^{n+1} &= f(\mathbf{x}, \theta t^{n+1} + (1 - \theta)t^n) \end{aligned}$$

and $0 \leq \theta \leq 1$.

Theorem 2. *For $\theta \geq 0.5$, the solution of the weighted difference scheme (17)-(18) satisfies the a priori estimate*

$$\|\mathbf{u}^{n+1}\|_a^2 + \|p^{n+1}\|_c^2 \leq \|\mathbf{u}^n\|_a^2 + \|p^n\|_c^2 + \frac{\tau}{2} \|f_\theta^{n+1}\|_{*,b}^2 \quad (19)$$

Proof. Let

$$\begin{aligned} \mathbf{u}_\theta^{n+1} &= \theta \mathbf{u}^{n+1} + (1 - \theta)\mathbf{u}^n, \\ v &= \frac{\mathbf{u}^{n+1} - \mathbf{u}^n}{\tau} \end{aligned}$$

in the equation for the displacement (17), then we have

$$a\left(\mathbf{u}_\theta^{n+1}, \frac{\mathbf{u}^{n+1} - \mathbf{u}^n}{\tau}\right) + g\left(p_\theta^{n+1}, \frac{\mathbf{u}^{n+1} - \mathbf{u}^n}{\tau}\right) = 0. \quad (20)$$

By analogy, substituting $q = p_\theta^{n+1}$ in the pressure equation (18), we obtain

$$\begin{aligned} c\left(\frac{p^{n+1} - p^n}{\tau}, p_\theta^{n+1}\right) + d\left(\frac{\mathbf{u}^{n+1} - \mathbf{u}^n}{\tau}, p_\theta^{n+1}\right) \\ + b(p_\theta^{n+1}, p_\theta^{n+1}) = (f_\theta^{n+1}, p_\theta^{n+1}). \end{aligned} \quad (21)$$

Adding (20) and (21), we get

$$a\left(\mathbf{u}_\theta^{n+1}, \frac{\mathbf{u}^{n+1} - \mathbf{u}^n}{\tau}\right) + c\left(\frac{p^{n+1} - p^n}{\tau}, p_\theta^{n+1}\right) + b(p_\theta^{n+1}, p_\theta^{n+1}) = (f_\theta^{n+1}, p_\theta^{n+1}).$$

Taking into account the inequality

$$(f_\theta^{n+1}, p_\theta^{n+1}) \leq \varepsilon \|p_\theta^{n+1}\|_b^2 + \frac{1}{4} \|f_\theta^{n+1}\|_{*,b}^2$$

then for $\varepsilon = 1$

$$a\left(\mathbf{u}_\theta^{n+1}, \frac{\mathbf{u}^{n+1} - \mathbf{u}^n}{\tau}\right) + c\left(\frac{p^{n+1} - p^n}{\tau}, p_\theta^{n+1}\right) \leq \frac{1}{4} \|f_\theta^{n+1}\|_{*,b}^2.$$

Here the right-hand side is estimated in the norm for the space adjoint to H_b using symbols $\|v\|_{*,b}$.

Using the identity

$$v_\theta^{n+1} = \theta v^{n+1} + (1 - \theta)v^n = \frac{v^{n+1} + v^n}{2} + \left(\theta - \frac{1}{2}\right)(v^{n+1} - v^n),$$

and employing that for symmetric bilinear form $d(u, v) = d(v, u)$ it is satisfied:

$$d(u + v, u - v) = d(u, u) - d(v, v),$$

we obtain the inequality

$$\begin{aligned} \frac{1}{2} (\|u^{n+1}\|_a^2 - \|u^n\|_a^2) + \frac{1}{2} (\|p^{n+1}\|_c^2 - \|p^n\|_c^2) \\ + \left(\theta - \frac{1}{2}\right) (\|u^{n+1} - u^n\|_a^2 + \|p^{n+1} - p^n\|_c^2) \leq \frac{\tau}{4} \|f_\theta^{n+1}\|_{*,b}^2. \end{aligned}$$

If $\theta \geq 0.5$, then the estimate (19) holds; this ensures stability with respect to the initial data and the right-hand side. \square

5. Additive schemes

Let H be a finite-dimensional Hilbert space, and \mathbb{B}, \mathbb{A} are linear operators in H . We introduce a space $H_{\mathcal{D}}$ with the inner product and norm:

$$(y, w)_{\mathcal{D}} = (\mathcal{D}y, w), \quad \|y\|_{\mathcal{D}} = (\mathcal{D}y, w)^{1/2}.$$

We consider a initial value problem for a system of linear ordinary differential equations: find $\mathbf{U}(t) \in H$ such that

$$\mathbb{B} \frac{d\mathbf{U}}{dt} + \mathbb{A}\mathbf{U} = \mathbf{F}, \quad t > 0, \quad (22)$$

$$\mathbb{B} = \begin{pmatrix} \mathcal{A} & \alpha \mathcal{G} \\ \alpha \mathcal{D} & S\mathcal{I} \end{pmatrix}, \quad \mathbb{A} = \begin{pmatrix} 0 & 0 \\ 0 & \mathcal{B} \end{pmatrix}, \quad (23)$$

with the initial conditions

$$\mathbf{U} = \mathbf{U}_0. \quad (24)$$

For the problem (22)-(24), we have the a priori estimate (14), which expresses the stability of the solution with respect to the initial data and the right-hand side.

In our problem, the computational complexity is associated with the operator \mathbb{B} at the time derivative. In this case, to decrease the computational complexity of the problem (22)-(24), we employ the additive representation:

$$\mathbb{B} = \mathbb{B}_0 + \mathbb{B}_1, \quad (25)$$

where we take \mathbb{B}_0 as an easily invertible operator; this can help us to decouple the problem.

Splitting schemes for the approximate solution of (22)-(24) will be constructed on the basis of the weighted difference schemes. The standard two-level weighted scheme for the problem (22)-(24) has the following form:

$$\mathbb{B} \frac{\mathbf{U}^{n+1} - \mathbf{U}^n}{\tau} + \mathbb{A} (\theta \mathbf{U}^{n+1} + (1 - \theta) \mathbf{U}^n) = \mathbf{F}^n, \quad n = 0, 1, \dots \quad (26)$$

where, for example,

$$\mathbf{F}^n = \mathbf{F}(\theta t^{n+1} + (1 - \theta)t^n),$$

and θ is the weight parameter.

To solve the problem (22)-(24) with the additive operator \mathbb{B} , we apply the following difference scheme:

$$\begin{aligned} \mathbb{B}_0 \frac{\mathbf{U}^{n+1} - \mathbf{U}^n}{\tau} + \mathbb{B}_1 \frac{\mathbf{U}^n - \mathbf{U}^{n-1}}{\tau} \\ + \mathbb{A} (\theta_1 \mathbf{U}^{n+1} + (1 - \theta_1 - \theta_2) \mathbf{U}^n + \theta_2 \mathbf{U}^{n-1}) = \mathbf{F}^n, \end{aligned} \quad (27)$$

$$n = 0, 1, \dots$$

Unlike (26), the scheme (27) is a three-level scheme with two weight factors θ_1 and θ_2 .

As the operators $\mathbb{B}_0, \mathbb{B}_1$ in (27), we can take the following representations:

$$\mathbb{B}_0 = \begin{pmatrix} \mathcal{A} & 0 \\ 0 & S\mathcal{I} \end{pmatrix}, \quad \mathbb{B}_1 = \begin{pmatrix} 0 & \alpha\mathcal{G} \\ \alpha\mathcal{D} & 0 \end{pmatrix}, \quad (28)$$

where the diagonal part of the operator \mathbb{B} is separated. In terms of numerical implementation, it is convenient to use the triangular splitting. The first case has the form:

$$\mathbb{B}_0 = \begin{pmatrix} \mathcal{A} & 0 \\ \alpha\mathcal{D} & S\mathcal{I} \end{pmatrix}, \quad \mathbb{B}_1 = \begin{pmatrix} 0 & \alpha\mathcal{G} \\ 0 & 0 \end{pmatrix}, \quad (29)$$

and the second one is represented as:

$$\mathbb{B}_0 = \begin{pmatrix} \mathcal{A} & \alpha\mathcal{G} \\ 0 & S\mathcal{I} \end{pmatrix}, \quad \mathbb{B}_1 = \begin{pmatrix} 0 & 0 \\ \alpha\mathcal{D} & 0 \end{pmatrix}. \quad (30)$$

In each of these decompositions, we have the part \mathbb{B}_0 that is easily invertible.

6. Regularized schemes

Now we consider some modified techniques, which often discussed in the literature [25, 26, 27, 28]. The undrained split method consists in imposing a constant fluid mass during the structure deformation [25, 26]. We set

$$p^{n+1} = p^n - \frac{\alpha}{S} \mathcal{D}(\mathbf{u}^{n+1} - \mathbf{u}^n),$$

then we substitute this into the displacement equation:

$$\mathcal{A} \mathbf{u}^{n+1} + \alpha \mathcal{G} p^n - \tau \frac{\alpha^2}{S} \mathcal{G} \mathcal{D} \frac{\mathbf{u}^{n+1} - \mathbf{u}^n}{\tau} = 0.$$

The equations become as follows:

$$\begin{aligned} \mathcal{A}\mathbf{u}^{n+1} + \alpha\mathcal{G}p^n - \tau\frac{\alpha^2}{S}\mathcal{GD}\frac{\mathbf{u}^{n+1} - \mathbf{u}^n}{\tau} &= 0, \\ S\frac{p^{n+1} - p^n}{\tau} + \alpha\mathcal{D}\frac{\mathbf{u}^{n+1} - \mathbf{u}^n}{\tau} + \mathcal{B}p^{n+1} &= f^n. \end{aligned} \quad (31)$$

The displacement equation in (31) can be generalized as a regularized scheme (see, e.g., [24, 29]):

$$\mathcal{A}\mathbf{u}^{n+1} + \alpha\mathcal{G}p^n + \beta\tau\mathcal{R}\frac{\mathbf{u}^{n+1} - \mathbf{u}^n}{\tau} = 0, \quad (32)$$

where, for the undrained split, we have

$$\mathcal{R} = -\frac{\mathcal{GD}}{S}, \quad \beta = \alpha^2.$$

The fixed stress split method consist in imposing constant volumetric mean total stress [25, 26]. We set

$$\mathcal{D}\mathbf{u}^{n+1} = \mathcal{D}\mathbf{u}^n + \alpha\frac{1}{K_{dr}}(p^{n+1} - p^n),$$

where K_{dr} is the constrained (drained) modulus:

$$K_{dr} = \frac{E(1 - \nu)}{(1 - 2\nu)(1 + \nu)}.$$

Substitution into the pressure equation leads to

$$S\frac{p^{n+1} - p^n}{\tau} + \alpha\mathcal{D}\frac{\mathbf{u}^n - \mathbf{u}^{n-1}}{\tau} + \left(\frac{\alpha^2}{K_{dr}}\frac{p^{n+1} - p^n}{\tau} - \frac{\alpha^2}{K_{dr}}\frac{p^n - p^{n-1}}{\tau} \right) + \mathcal{B}p^{n+1} = f^n,$$

and now we get

$$\begin{aligned} \mathcal{A}\mathbf{u}^{n+1} + \alpha\mathcal{G}p^{n+1} &= 0, \\ S\frac{p^{n+1} - p^n}{\tau} + \alpha\mathcal{D}\frac{\mathbf{u}^n - \mathbf{u}^{n-1}}{\tau} &+ \left(\frac{\alpha^2}{K_{dr}}\frac{p^{n+1} - p^n}{\tau} - \frac{\alpha^2}{K_{dr}}\frac{p^n - p^{n-1}}{\tau} \right) + \mathcal{B}p^{n+1} = f^n. \end{aligned} \quad (33)$$

Similarly, we can generalize the pressure equation in (33) as a regularized scheme [24, 29]:

$$S\frac{p^{n+1} - p^n}{\tau} + \alpha\mathcal{D}\frac{\mathbf{u}^n - \mathbf{u}^{n-1}}{\tau} + \beta\tau\mathcal{R}\frac{p^{n+1} - 2p^n + p^{n-1}}{\tau^2} + \mathcal{B}p^{n+1} = f^n, \quad (34)$$

where, for the fixed stress split, we have

$$\mathcal{R} = \frac{1}{K_{dr}}, \quad \beta = \alpha^2.$$

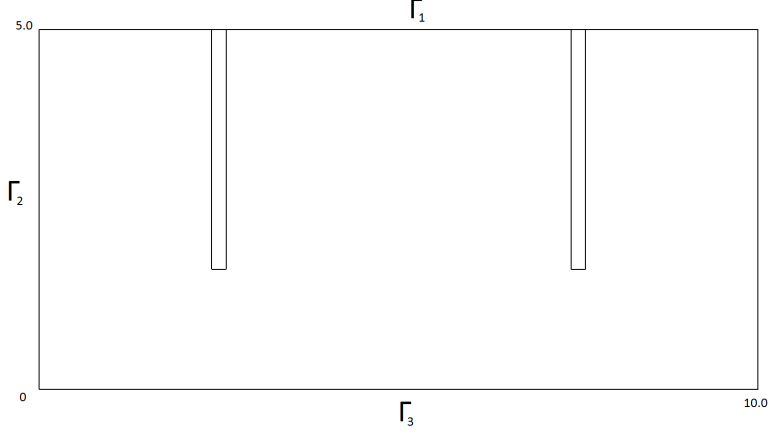


Figure 1: Computational domain

7. Numerical tests for poroelasticity problems

Let us compare the additive scheme (27) with the additive operator

$$\mathbb{B} = \mathbb{B}_0 + \mathbb{B}_1,$$

and the regularized schemes (32), (34) on the tests, where coefficients are typical for poroelasticity problems. For numerical implementation, we use **Gmsh** [32] for mesh generation and **Paraview** [33] for visualization of numerical results. Our code is based on the library for scientific computations **FEniCS** [31]. Two test cases have been predicted.

Figure 1 presents the computational domain whereas Figure 2 demonstrates two meshes used for the numerically solving poroelasticity problem. Parameters of problem are presented in Table 1 for Test 1 and Test 2. We use the following boundary conditions:

$$\begin{aligned} \sigma_{x_1} &= 0, & \sigma_{x_2} &= 0, & \mathbf{x} &\in \Gamma_1, \\ u_{x_1} &= 0, & \sigma_{x_2} &= 0, & \mathbf{x} &\in \Gamma_2, \\ u_{x_1} &= 0, & u_{x_2} &= 0, & \mathbf{x} &\in \Gamma_3. \end{aligned}$$

The time steps $\tau = 0.1$ day and $t_{max} = 3$ days were used on the finest spatial mesh with 40000 cells. The pressure field along with the displacement and stress (von Mises) distributions are depicted in Fig. 3 as the upper, middle and lower isocontours, respectively, for the second test case.

To compare the errors produced by the above schemes, we use the fully coupled method with the finest mesh of 40000 cells and time step $\tau = 0.1$ day in order to calculate the benchmark solution for evaluating the error. For error comparison we use

$$\varepsilon_p = \|p_e - p\|, \quad \|p_e - p\|^2 = \int_{\Omega} (p_e - p)^2 d\mathbf{x},$$

Parameter	Symbol	Test 1	Test 2
Biot modulus	M	5.0 GPa	50.0 GPa
Shear modulus	μ	5.0 GPa	15.0 GPa
Lame constant	λ	5.0 GPa	10.0 GPa
Absolute permeability	k	10^{-17} m^2	10^{-18} m^2
Fluid viscosity	ν	0.001 Pa/sec	0.001 Pa/sec
Initial pressure	p_0	10.0 MPa	10.0 MPa
Injector pressure	p_i	10.01 MPa	10.01 MPa
Producer pressure	p_p	9.99 MPa	9.99 MPa

Table 1: Problem properties

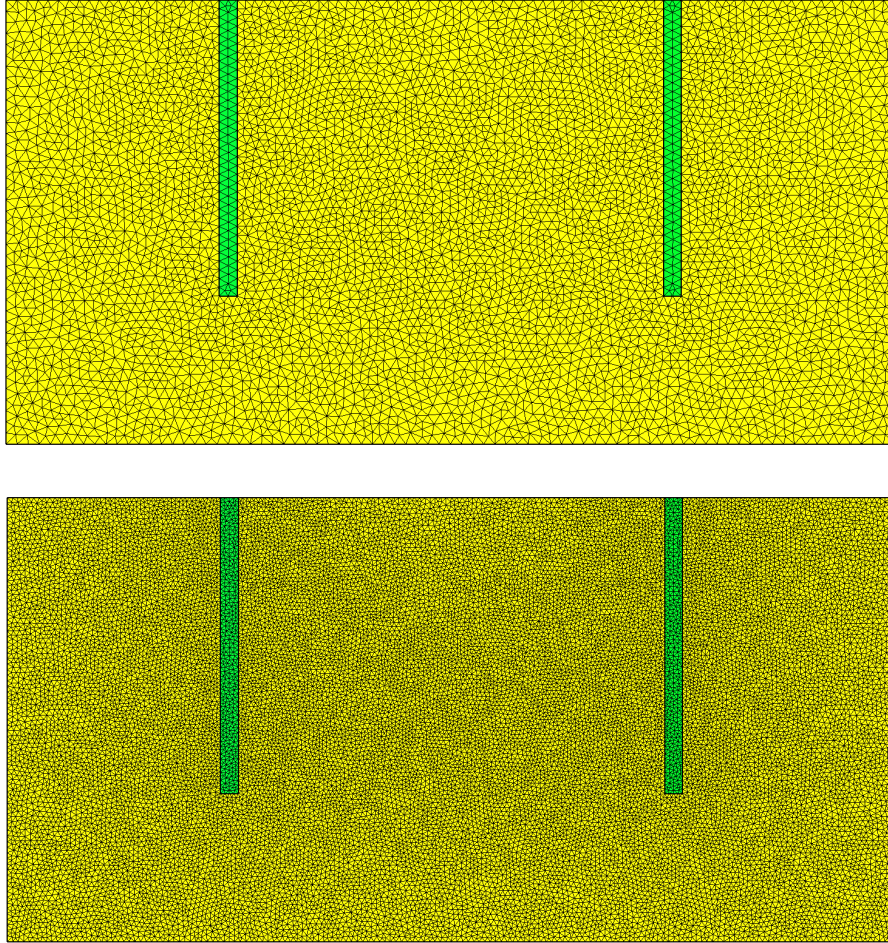


Figure 2: Computational grids (10000 and 40000 cells)

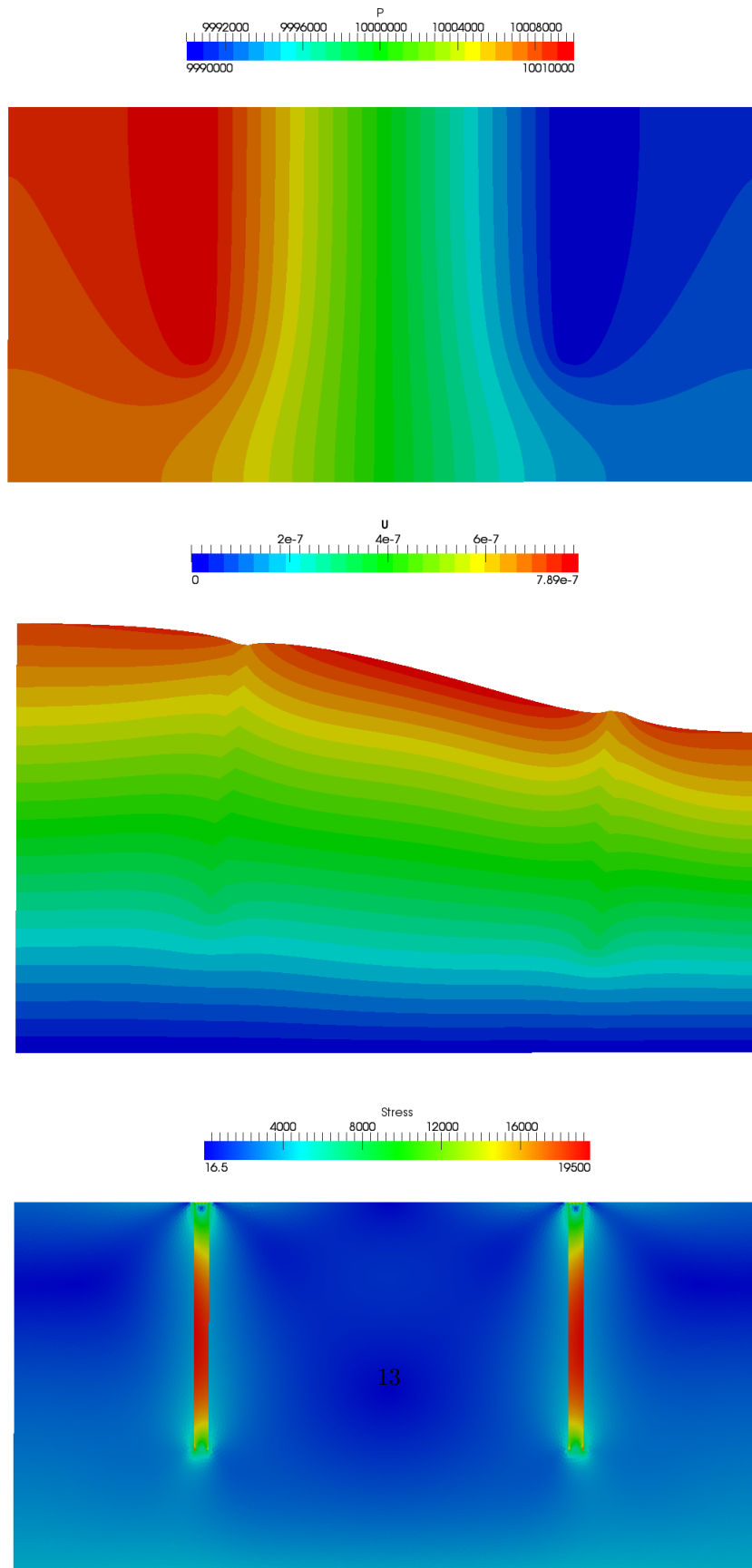


Figure 3: Pressure (upper), displacement ($\times 10^6$) (middle) and stress (lower) distributions

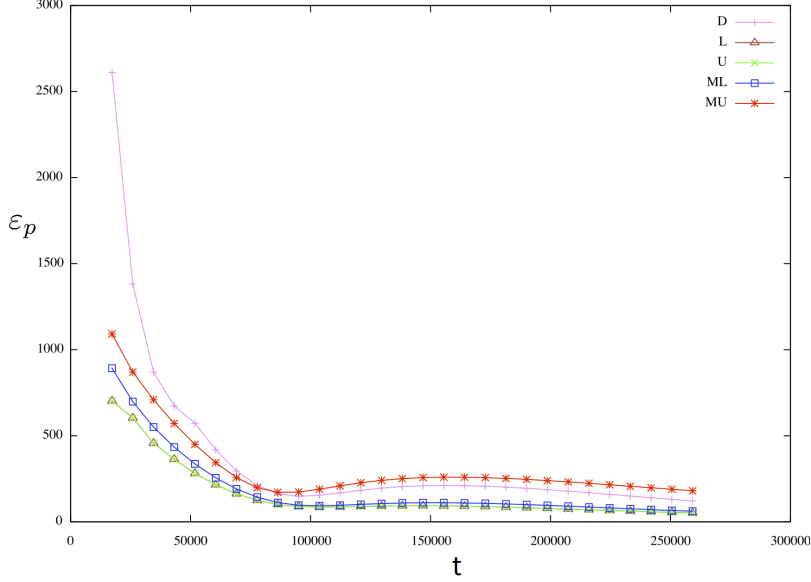


Figure 4: Comparison of the error for the pressure (Test 1)

where p_e is the benchmark solution of pressure and p – calculated pressure. Figures 4 and 5 demonstrate the errors obtained using the splitting schemes (28), (29), (30) (D, L, U on Fig. 4 and Fig. 5) and modifications (32), (34) (ML, MU on Fig. 4 and Fig. 5) on the mesh of 10000 cells for Tests 1 and 2, respectively.

For Test 2, We observe numerical instability for our additive representations of the operator \mathbb{B} . But applying the modified schemes for Test 2, we obtain the stable solution. As for Test 1, all schemes do work.

8. Three-dimensional poroelasticity problem

Next, we consider a three-dimensional reservoir with one vertical injection well and four horizontal production wells. The reservoir domain is shown in Fig. 6 with plotted wells. The domain is as large as $200 \times 200 \times 20$ m. The production and injection wells work with $p_p = 9.9975$ MPa and $p_i = 10.001$, respectively. The rock and fluid parameters of the problem are similar to Test 2 from the previous section.

Three meshes of different quality were used for predictions (see Fig. 7 for the coarse (upper), medium (middle) and fine (lower picture) grid). The numbers of vertices, cells, and degrees of freedom (dof) of p , \mathbf{u} , and \mathbf{w} for each mesh are given in Table 2. We see that the number of dofs for the displacement field \mathbf{u} is much higher than the dofs number for the pressure field p . This results from the fact that of the quadratic vector element and the linear scalar element are used for discretization of the displacement and pressure, respectively. For the fully coupled method, we search the combined vector \mathbf{w} that is sum of \mathbf{u} and p .

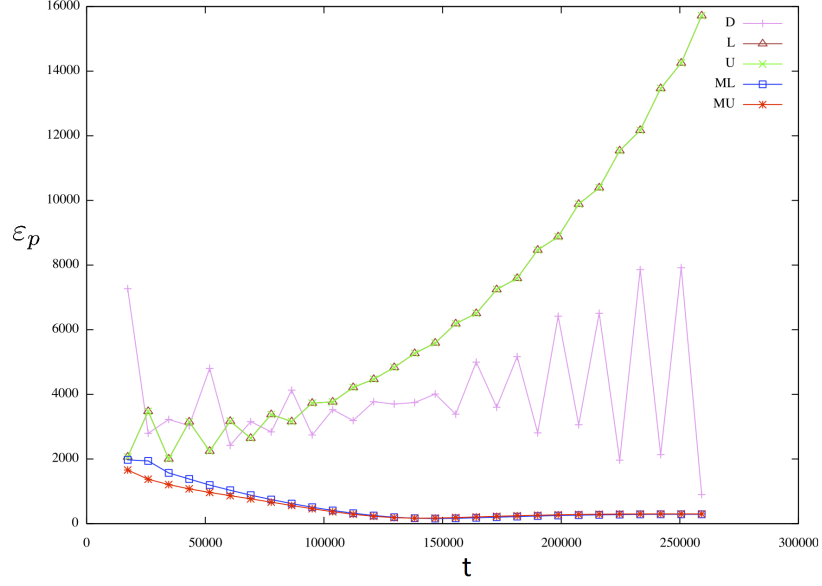


Figure 5: Comparison of the error for the pressure (Test 2)

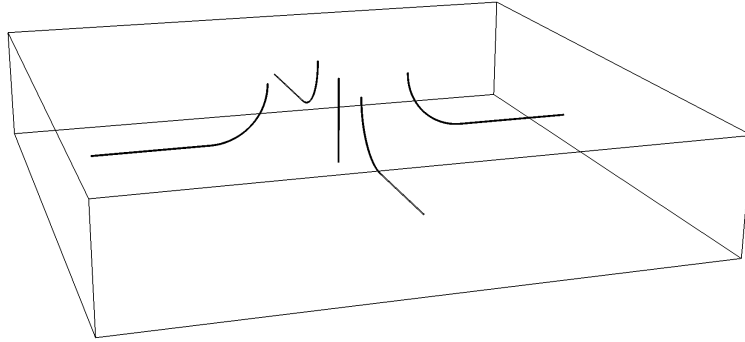


Figure 6: Reservoir with plotted wells

	mesh1	mesh2	mesh3
Vertices	19005	30502	78956
Cells	95088	146541	376056
Number of p dof	19005	30502	78956
Number of \mathbf{u} dof	415287	655179	1691586
Number of \mathbf{w} dof	434292	685681	1770542

Table 2: Parameters of meshes

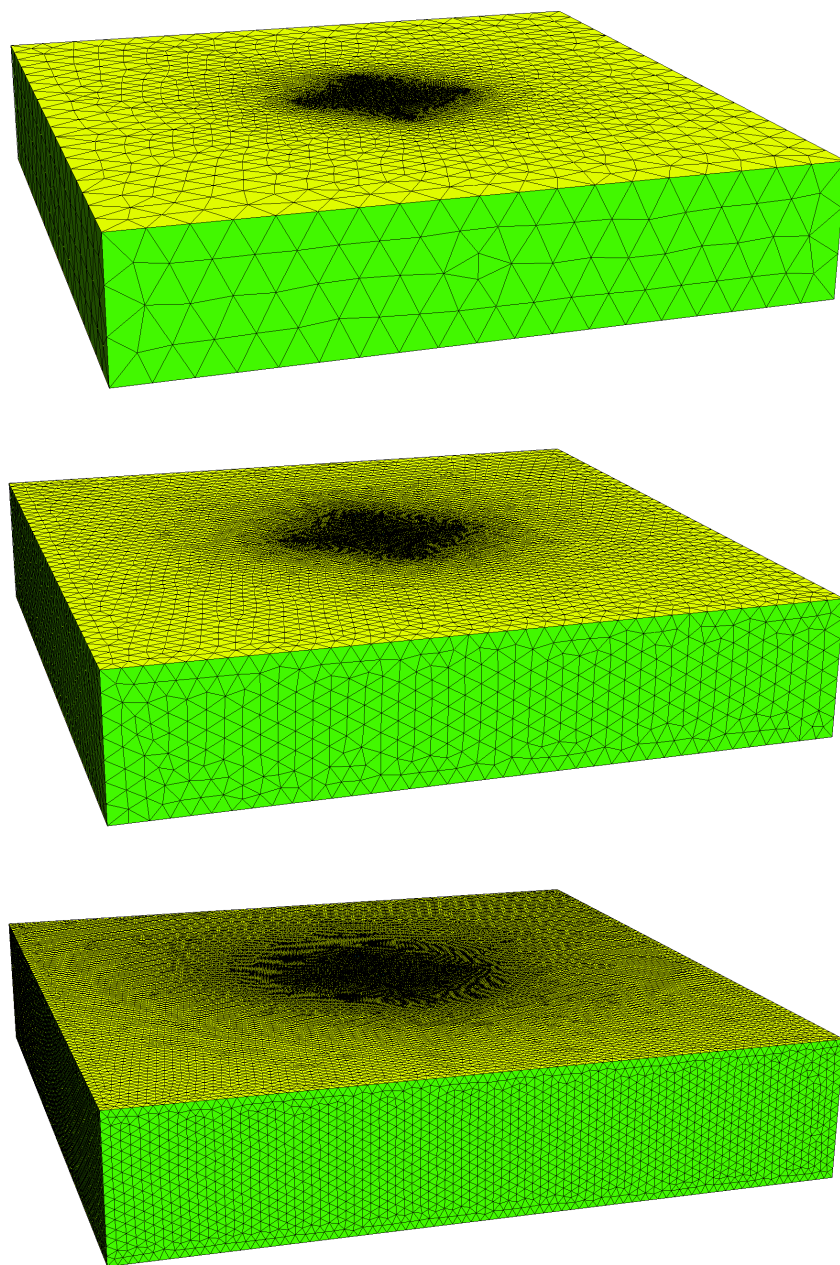


Figure 7: Computational meshes: the coarse (upper), medium (middle) and fine (lower picture) grid

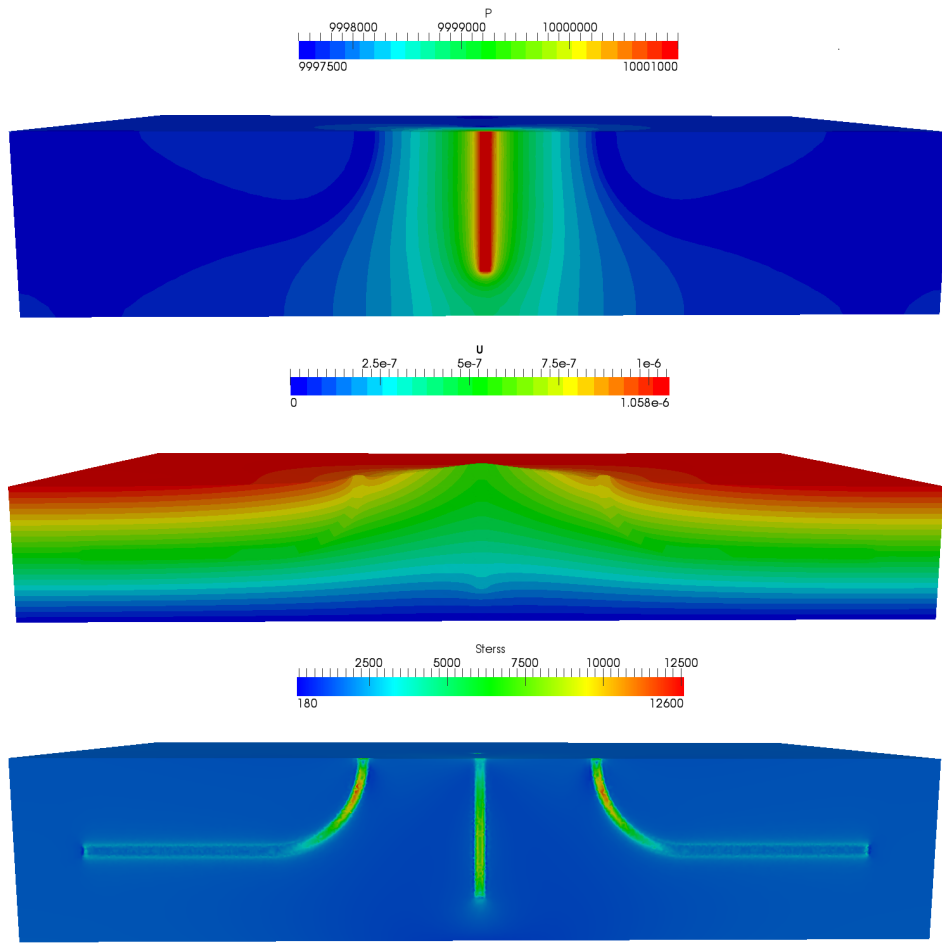


Figure 8: Pressure (upper), displacement ($\times 5.0 \cdot 10^6$) (middle) and stress (lower) distributions

np	mesh1		mesh2		mesh3	
	coupled	split	coupled	split	coupled	split
1	4869.57	3129.18	9140.62	6174.50	40918.40	32566.40
2	2101.24	1247.07	3826.16	2438.96	16813.20	11360.30
4	1020.60	572.50	1647.10	1059.33	5959.41	4285.02
8	598.61	376.68	956.65	624.52	3105.15	2177.98
16	451.77	322.40	635.43	492.61	1768.68	1235.90
32	230.23	200.69	383.93	312.09	1015.04	657.06

Table 3: Comparison of coupled and RU-split methods run times

The results of numerical experiments are presented in Fig. 8. The time step $\tau = 1$ day and the maximum time $T_{max} = 30$ day were used. The generalized minimal residual method (GMRES) with incomplete LU-factorization preconditioner (ILU) was chosen as the linear solver for of both schemes. Numerical experiments on a different number of processors were conducted. Calculation times for the coupled scheme and the splitting schemes (MU) are shown in Table 3. A good parallelization efficiency is observed.

The parallel code was run on a cluster *Arian Kuzmin* of NorthEastern Federal University. The cluster consists of 160 computing nodes, each node has two 6-core processors Intel Xeon X5675 3.07 GHz with 48 GB RAM.

9. Conclusions

1. Stability estimates of weighted schemes for the coupled system of equations are obtained for the differential and discrete problem using Samarskii's theory of stability for operator-difference schemes.
2. Splitting schemes are constructed using an additive representation of the operator at the time derivative. Undrained and fixed stress split methods are presented as regularized schemes.
3. It was found that the additive schemes do not always work, and for some problem parameters, we need to use the regularized schemes.
4. For solving the three-dimensional problem, parallel computations were performed using the standard technique. They demonstrate good parallelization efficiency for both the coupled and splitting schemes.

References

- [1] M. A. Biot, General theory of three-dimensional consolidation, Journal of applied physics 12 (2) (1941) 155–164.
- [2] H. Wang, Theory of Linear Poroelasticity with Applications to Geomechanics and Hydrogeology, Princeton University Press, 2000.
- [3] S. E. Minkoff, C. M. Stone, S. Bryant, M. Peszynska, M. F. Wheeler, Coupled fluid flow and geomechanical deformation modeling, Journal of Petroleum Science and Engineering 38 (1) (2003) 37–56.
- [4] A. Meirmanov, Mathematical Models for Poroelastic Flows, Springer, 2014.
- [5] M. A. Biot, Thermoelasticity and irreversible thermodynamics, Journal of Applied Physics 27 (3) (1956) 240–253.

- [6] J. Lubliner, Plasticity theory, Dover Publications, 2008.
- [7] J. C. Simo, T. J. R. Hughes, Computational inelasticity, New York, 1998.
- [8] W. Nowacki, Dynamic problems of thermoelasticity, Springer, 1975.
- [9] T. J. R. Hughes, The finite element method: linear static and dynamic finite element analysis, DoverPublications. com, 2012.
- [10] O. C. Zienkiewicz, R. L. Taylor, J. Z. Zhu, The Finite Element Method: Its Basis and Fundamentals, Butterworth-Heinemann, 2005.
- [11] J. B. Haga, H. Osnes, H. P. Langtangen, On the causes of pressure oscillations in low-permeable and low-compressible porous media, International Journal for Numerical and Analytical Methods in Geomechanics 36 (12) (2012) 1507–1522.
- [12] S. E. Minkoff, N. M. Kridler, A comparison of adaptive time stepping methods for coupled flow and deformation modeling, Applied mathematical modelling 30 (9) (2006) 993–1009.
- [13] F. Armero, Formulation and finite element implementation of a multiplicative model of coupled poro-plasticity at finite strains under fully saturated conditions, Computer methods in applied mechanics and engineering 171 (3) (1999) 205–241.
- [14] I. Babuška, The finite element method with lagrangian multipliers, Numerische Mathematik 20 (3) (1973) 179–192.
- [15] F. Brezzi, On the existence, uniqueness and approximation of saddle-point problems arising from lagrangian multipliers, ESAIM: Mathematical Modelling and Numerical Analysis-Modélisation Mathématique et Analyse Numérique 8 (R2) (1974) 129–151.
- [16] F. Brezzi, M. Fortin, Mixed and hybrid finite element methods, Springer-Verlag New York, Inc., 1991.
- [17] R. J. LeVeque, Finite difference methods for ordinary and partial differential equations. Steady-state and time-dependent problems, Society for Industrial Mathematics, 2007.
- [18] U. M. Ascher, Numerical methods for evolutionary differential equations, Society for Industrial Mathematics, 2008.
- [19] F. Gaspar, F. Lisbona, P. Vabishchevich, A finite difference analysis of biot’s consolidation model, Applied numerical mathematics 44 (4) (2003) 487–506.
- [20] F. J. Lisbona, P. N. Vabishchevich, Operator-splitting schemes for solving unsteady elasticity problems, Comput. Methods Appl. Math. 1 (2) (2001) 188–198.
- [21] A. A. Samarskii, The theory of difference schemes, Marcel Dekker, New York, 2001.
- [22] A. A. Samarskii, P. P. Matus, P. N. Vabishchevich, Difference schemes with operator factors, Kluwer Academic Pub, 2002.
- [23] G. I. Marchuk, Splitting and alternating direction methods, in: P. G. Ciarlet, J.-L. Lions (Eds.), Handbook of Numerical Analysis, Vol. I, North-Holland, 1990, pp. 197–462.
- [24] P. N. Vabishchevich, Additive operator-difference schemes. Splitting schemes, de Gruyter, 2013.
- [25] J. Kim, Sequential methods for coupled geomechanics and multiphase flow, Ph.D. thesis, Stanford University (2010).
- [26] A. Mikelic, M. F. Wheeler, Convergence of iterative coupling for coupled flow and geomechanics, Computational Geosciences (2013) 1–7.
- [27] F. Armero, J. C. Simo, A new unconditionally stable fractional step method for non-linear coupled thermomechanical problems, International Journal for numerical methods in Engineering 35 (4) (1992) 737–766.
- [28] B. Jha, R. Juanes, A locally conservative finite element framework for the simulation of coupled flow and reservoir geomechanics, Acta Geotechnica 2 (3) (2007) 139–153.
- [29] A. A. Samarskii, Regularization of difference schemes, USSR Computational Mathematics and Mathematical Physics 7 (1) (1967) 79–120.
- [30] A. A. Samarskii, E. S. Nikolaev, Numerical methods for grid equations. Vol. II, Birkhauser Verlag, Basel, 1989.
- [31] A. Logg, K.-A. Mardal, G. Wells, Automated solution of differential equations by the finite element method: The fenics book, Vol. 84, Springer, 2012.
- [32] C. Geuzaine, J.-F. Remacle, Gmsh: A 3-d finite element mesh generator with built-in pre-and post-processing facilities, International Journal for Numerical Methods in Engineering 79 (11) (2009) 1309–1331.
- [33] A. Henderson, J. Ahrens, C. Law, The ParaView Guide, Kitware Clifton Park, NY, 2004.